Diel variability of heterotrophic bacterial production and underwater UV doses in the eastern South Pacific

France van Wambeke, M. Tedetti, S. Duhamel, Richard Sempere

Diel variability of heterotrophic bacterial production and underwater UV doses in the eastern South Pacific

France Van Wambeke[1,*], Marc Tedetti[1], Solange Duhamel[1,2], Richard Sempéré[1]

[1]**Laboratoire de Microbiologie, Géochimie et Ecologie Marines (LMGEM), CNRS, UMR 6117, Université de la Méditerranée, Campus de Luminy - Case 901, 13288 Marseille cedex 9, France**

[2]***Present address:*** **C-MORE, Department of Oceanography, University of Hawaii, 1000 Pope Road, MSB205 Honolulu, Hawaii 96822, USA**

ABSTRACT: Diel variability of heterotrophic bacterial production (BP) was investigated in the eastern South Pacific from October to December 2004. Three sites differing by their trophic status were studied: Marquesas Islands, the center (GYR) and the eastern South Pacific Gyre. By using a Lagrangian approach and high frequency measurements, an important increase (2- to 4-fold) in BP was observed at the 3 sites during the afternoon–sunset period within surface layers. To evaluate the impact of solar UV radiation on this variability, we determined, from *in situ* optical measurements, the mean UV-B (at 305 nm) and UV-A (at 380 nm) doses received within the mixed layer at a daily scale. At GYR, the doses were as high as 0.3 and 11 kJ m^{-2} nm^{-1} for the whole day, respectively due to high surface irradiances and very low light attenuations in the water column. The UV-B/UV-A tri-hourly dose ratios (Q) displayed substantial variations during the daytime, with highest values recorded during the periods 9:00 to 12:00 h or 12:00 to 15:00 h. The negative linear correlation observed between Q and BP in the surface waters of GYR suggests that changes in the balance between DNA damages and photorepairs (reflected by changes in the Q-ratio) could have a significant influence on the diel variability of BP in open oceans. However, assessing the effects of UV radiation on diel variability of BP through an *in situ* measurement approach, independently from other causes like availability of resources, is not so evident, even in these clearest waters of the world ocean.

KEY WORDS: Eastern South Pacific · Heterotrophic bacterial production · Diel variability · Ultraviolet radiation · UV-B and UV-A doses · Mixed layer · Leucine

INTRODUCTION

The context of climate change and stratospheric ozone depletion has stimulated interest in investigating the effects of solar radiation, and more specifically ultraviolet radiation (UVR: 280 to 400 nm), on aquatic ecosystems (Häder et al. 2003). In the surface waters, UVR can significantly affect heterotrophic bacteria that are too small to efficiently use UVR-absorbing pigments as sunscreens (Garcia-Pichel 1994). Ultraviolet-B (UV-B: 280 to 315 nm) is strongly absorbed by cellular DNA, altering the DNA structure and producing damages such as cyclobutane pyrimidine dimers (CPDs) (Häder & Sinha 2005). Many studies have reported the inhibition of heterotrophic bacterial production (BP) after exposure of natural microbial assemblages to UV-B and the subsequent production of CPDs (Aas et al. 1996, Jeffrey et al. 1996). On the other hand, DNA damages can be repaired through 2 pathways: (1) photoenzymatic repairs (PERs) via the action of photolyase, induced by both ultraviolet-A (UV-A: 315 to 400 nm) and photosynthetically available radiation (PAR: 400 to 700 nm) and (2) excision repairs that occur in the dark (Häder & Sinha 2005). PERs have been observed in nat-

ural assemblages and bacterial cultures exposed to artificial UV-B after secondary irradiation with UV-A and PAR. It appears that UV-A is more efficient than PAR in inducing photoreactivation (Kaiser & Herndl 1997, Joux et al. 1999). Therefore, the rates of CPDs production and PERs in marine microbial assemblages may be related to the UV-B and UV-A doses (irradiances integrated over time) received by cells (Boelen et al. 2001). In the surface ocean, the intensity of UV-B and UV-A doses for a given time period depends on several parameters: (1) the level of surface UV-B and UV-A irradiances, (2) the attenuation of these surface irradiances in the water column, which is mainly controlled by chromophoric dissolved organic matter (CDOM) (Diaz et al. 2000) and (3) the depth of the mixed layer (Z_m), i.e. the depth at which cells can be transported within the upper water column (Boelen et al. 2001).

The French project BIogeochemistry and Optics SOuth Pacific Experiment (BIOSOPE) was dedicated to a multidisciplinary exploration of the eastern South Pacific including the hyper-oligotrophic South Pacific Gyre (SPG) as well as its western (Marquesas Islands) and eastern (Chilean upwelling) borders in late 2004 (Claustre et al. 2008a). As in other subtropical regions, the eastern South Pacific is subjected to high surface UV-B and UV-A irradiances due to the small solar zenith angle (SZA) and the relatively low ozone amounts (200 to 300 Dobson Units) (TOMS satellite data; http://toms.gsfc.nasa.gov/ozone/ozone_v8.html). Moreover, the very low content in chlorophyll *a* (chl *a*) and CDOM in the highly stratified surface waters of the SPG allow for a very deep penetration of UVR (Morel et al. 2007, Tedetti et al. 2007). In the surface layers of this oceanic area, nitrogen (N) has been shown to be a common factor limiting both phytoplankton and heterotrophic bacteria (Van Wambeke et al. 2008a). Consequently, in the SPG, the diel variability of BP could be particularly intense, influenced by the UV-B and UV-A doses received within Z_m (i.e. the balance between DNA damages and repairs), but also by the trophic dependence of heterotrophic bacteria on phytoplankton exudates and/or regeneration processes.

The first goal of the present study was to determine the diel variability of BP as well as underwater UV doses received at fixed depths and within the mixed layer in the eastern South Pacific at 3 selected sites differing by their trophic status: the Marquesas Islands, and the center and the eastern border of the SPG. The second goal was to examine whether, in the most oligotrophic and transparent waters of the world ocean, a causal relationships between UVR and BP can be inferred simply from high frequency *in situ* measurements of BP and UV doses, without processing any experimental set-up in bottles.

MATERIALS AND METHODS

Sampling strategy

The BIOSOPE campaign was conducted from 24 October to 11 December, 2004 aboard RV 'l'Atalante' in the eastern South Pacific. The cruise consisted of 'short' and 'long' sites. Diel variability of BP was estimated at 3 of these long sites: MAR (vicinity of Marquesas Islands), GYR (center of the SPG) and EGY (eastern border of the SPG). These sites differed in terms of physical and biological characteristics (Claustre et al. 2008a; our Table 1). CTD casts were performed every 3 h during successive days (i.e. at local times 00:00, 03:00, 06:00, 09:00, 12:00, 15:00, 18:00 and 21:00 h). Samples were collected from a CTD rosette fitted with twenty 12 l Niskin bottles equipped with Teflon rings to avoid carbon contaminations. Samples were processed within 0.5 h of collection. For the study of BP diel variability, 9 to 10 levels were sampled along the water column down to 170 m at MAR, 280 m at GYR and 250 m at EGY. The period of high frequency sampling for BP measurements was 36 h at MAR on 27 to 28 October (every 3 h), 48 h at GYR on 12 to 14 November (every 3 h) and 42 h at EGY on 26 to 28 November (every 6 h).

Determination of the mixed layer depth

Z_m was determined for each CTD cast and at all sites. It corresponded to the average of the following 4 measures: the depths at which the density difference with that of surface reached (1) 0.05 kg m^{-3} and (2) 0.1 kg m^{-3}; and the depths at which the density gradient reached (3) 0.01 kg m^{-4} and (4) 0.02 kg m^{-4}. This average value based on 4 different criteria occasionally exhibited large variability, particularly at GYR where the density profile showed a succession of pycnoclines not very well contrasted (see Fig. 1). In addition, slight increases in temperature in the upper surface layers during the evening led to micro-stratification within the 10 m subsurface layers. Therefore, for these CTD casts, we reconsidered Z_m values using only the first criterion and neglecting the first 10 m micro-gradient. Estimates of Z_m at GYR must, thus, be considered with caution.

Heterotrophic bacterial production

BP was determined by [^{3}H] leucine incorporation, applying the centrifugation method (Smith & Azam 1992). Duplicate 1.5 ml subsamples and one trichloroacetic acid-killed blank (5% final concentration) were

incubated (2 h in the dark at the respective *in situ* temperatures) with a final concentration of 20 nM added leucine (mixture of 6.6 nM [4,5-^{3}H] leucine, Amersham, 160 Ci mmol^{-1} and 13 nM 'cold' leucine). The leucine-carbon conversion factor was 1.5 kg C mol^{-1} leucine incorporated. Assumptions of (1) linearity of incorporation of leucine during time of incubation and (2) an isotopic dilution factor set to 1 with the 20 nM final leucine concentration added were checked previously in a companion paper (Van Wambeke et al. 2008b). Bovine serum albumin was added before the first centrifugation (100 mg l^{-1} final concentration) as it gave results compatible with the filtration technique (see details in Van Wambeke et al. 2008b). Error associated with the variability between replicate measurements (half the difference between the 2 replicates) averaged 13 and 6% for BP values less and more than 10 ng C l^{-1} h^{-1}, respectively.

UVR measurements and determination of UV-B and UV-A doses

Two profiles of downward irradiance ($E_{dZ,\lambda}$ in µW cm^{-2} nm^{-1}) were made at each site close to solar noon using a Satlantic MicroPro free-fall profiler equipped with OCR-504 downward irradiance sensors in the UV-B (305 nm) and UV-A (325, 340 and 380 nm) spectral domains. Surface irradiance ($E_{d0^+,\lambda}$ in µW cm^{-2} nm^{-1}) was simultaneously measured at the same channels on the ship deck using other OCR-504 sensors to account for the variations of cloud conditions during the cast as well as to monitor UV-B and UV-A irradiances during the day time. For in-water and in-air sensors, the Full-Width Half-Maximum (FWHM) of the channels was 2 nm for 305, 325 and 340 nm, and 10 nm for 380 nm. A detailed description of UVR measurements is given in Tedetti et al. 2007.

We determined UV-B and UV-A doses at MAR (28 Oct), GYR (13 Nov) and EGY (26 Nov) at fixed depths into the water column ($H_{Z,\text{UV-B}}$ and $H_{Z,\text{UV-A}}$ in kJ m^{-2} nm^{-1}) as well as mean UV-B and UV-A doses received within the mixed layer ($H_{m,\text{UV-B}}$ and $H_{m,\text{UV-A}}$ in kJ m^{-2} nm^{-1}). The wavelengths 305 nm (UV-B) and 380 nm (UV-A) were used as biologically effective wavelengths for the induction of CPDs and PERs, respectively (Häder & Sinha 2005). $H_{Z,\text{UV-B}}$ and $H_{Z,\text{UV-A}}$ were assessed using the following formula:

$$H_{Z,\lambda} = H_{0^-,\lambda} \times e^{(-K_{d\lambda} \times Z)} \quad (1)$$

where $H_{0^-,\lambda}$ is the dose beneath the sea surface (kJ m^{-2} nm^{-1}), $K_{d\lambda}$ is the diffuse attenuation coefficient for downward irradiance (m^{-1}), Z is the depth considered (m) and λ is the wavelength (305 or 380 nm). Here we calculated $H_{Z,\text{UV-B}}$ and $H_{Z,\text{UV-A}}$ at 5 and 10 m depth (i.e. $H_{5m,\text{UV-B}}$, $H_{5m,\text{UV-A}}$, $H_{10m,\text{UV-B}}$, and $H_{10m,\text{UV-A}}$). Conversely, $H_{m,\text{UV-B}}$ and $H_{m,\text{UV-A}}$ were evaluated using an equation taking into account the depth of the mixed layer (Boelen et al. 2000):

$$H_{m,\lambda} = H_{0^-,\lambda} \times [1 - e^{(-K_{d\lambda} \times Z_m)}] / (K_{d\lambda} \times Z_m) \quad (2)$$

where Z_m is the mixed layer depth (m) that corresponds to the mean of the 2 Z_m observed at the beginning and at the end of the exposure period considered for the dose calculation (3 h, see below). These 2 Z_m values were determined from CTD profiles as described above. All the doses were computed over tri-hourly exposure periods: 06:00–09:00 h, 09:00–12:00 h, 12:00–15:00 h and 15:00–18:00 h (local time). These tri-hourly doses were summed to obtain daily (6:00–18:00 h) doses. The detailed methodology for the appraisal of $H_{0^-,\lambda}$ and $K_{d\lambda}$, which are both used in Eqs. (1) and (2), is as follows.

$H_{0^-,\lambda}$ (dose beneath the sea surface) was obtained by integrating downward irradiance beneath the sea surface ($E_{d0^-,\lambda}$ in µW cm^{-2} nm^{-1}) over the exposure period: (t, time)

$$H_{0^-,\lambda} = \Sigma\, E_{d0^-,\lambda}\, \Delta t \quad (3)$$

$E_{d0^-,\lambda}$ was theoretically computed from measurement of $E_{d0^+,\lambda}$ using the formula:

$$E_{d0^-,\lambda} = E_{d0^+,\lambda} / (1 + \alpha) \quad (4)$$

where α is ocean surface albedo determined using a 'look up table' available online at http://www-cave.larc.nasa.gov/cave/ (Jin et al. 2004). This look up table, based on the validated Coupled Ocean–Atmosphere Radiative Transfer model, requires 4 input parameters to retrieve α at any spectral band of the solar spectrum: SZA, wind speed, aerosol/cloud optical depth and chl *a* concentration (Jin et al. 2004). SZA (°) was retrieved every hour from the T. Dibble SZA calculator (www.esf.edu/chemistry/dibble/atmoschemcalc.htm) that uses location (latitude, longitude), date (day, month), and universal time (UT) of measurements. Wind speed (knots converted into m s^{-1}) was measured continuously on board. At MAR and GYR (cloudless days), aerosol optical depth at 550 nm was estimated at 0.15 and 0.05, respectively (Myhre et al. 2005). At EGY (cloudy day), cloud optical depth at 500 nm was assessed at 15 (second highest value in the table). Total chl *a* concentrations (TChla, mg m^{-3}) were used from Ras et al. (2008). Therefore, α, computed every hour at 305 and 380 nm, was highly variable at MAR (ranging from 0.050 at 12:00 h to 0.097 at 17:00 h) and GYR (ranging from 0.057 at 12:00 h to 0.108 at 17:00 h), and very stable at EGY (~0.068 from 06:00–18:00 h).

$K_{d\lambda}$ was determined at each station close to solar noon from the slope of the linear regression of the log-transformed downward irradiance versus depth:

$$K_{d\lambda} = \ln (E_{d0^-,\lambda} / E_{dZ,\lambda}) / Z \quad (5)$$

where Z was 15 m (MAR) or 30 m (GYR and EGY). Correlation coefficients (r) of the linear regressions were > 0.99 for the 3 sites. Because of the SZA increasing during the day time, $K_{d\lambda}$, measured only close to solar noon, was corrected for the geometric condition of the light field by dividing by Gordon's (1989) correction factor ($D_{o\lambda}$):

$$D_{o\lambda} = (f_\lambda / \cos SZA_0^-) + 1.197 \times (1 - f_\lambda) \quad (6)$$

where f_λ is the direct fraction of global irradiance and SZA_0^- is the SZA beneath the sea surface. Since diffuse irradiance was not measured, we used average f_λ values available from literature for the UV spectral domain (Kuhn et al. 1999): 0.36 and 0.57 at 305 and 380 nm, respectively, for cloudless days (MAR and GYR). To facilitate the calculation, EGY was considered with an overcast sky, i.e. with no direct radiation (f_λ = 0.00). SZA_0^- was obtained by applying Snell's law to SZA above water:

$$SZA_0^- = \sin^{-1} (\sin SZA / n) \quad (7)$$

where n (~1.34) is the refraction index of water. $D_{o\lambda}$, which is wavelength dependent, was computed every hour at 305 and 380 nm and then averaged over the trihourly periods. $D_{o\lambda}$ ranged from 1.11 (12:00–15:00 h) to 1.30 (06:00–09:00 h and 15:00–18:00 h) at MAR and GYR, whereas it was constant (1.197) at EGY. Assuming a vertical homogeneity of the distribution of attenuating substances and organisms over the depth interval 0^- m to TChla maximum (Tedetti et al. 2007; our Table 1), the 10% irradiance depth ($Z_{10\%\lambda}$ in m), which is the depth where the downward irradiance is 10% of its surface value, was extrapolated from $K_{d\lambda}$:

$$Z_{10\%\lambda} = \ln(10) / K_{d\lambda} = 2.30 / K_{d\lambda} \quad (8)$$

RESULTS

Physical, biological and optical characteristics at the 3 sites

The main physical and biological characteristics of the 3 sites studied for diel variability of BP are presented in Table 1. There were significant differences between the 3 sites for most of the parameters: temperature, Z_m, depth of the euphotic zone (Z_e), depth of TChla maximum and concentration of TChla at this depth (Table 1). Mean surface temperature (5 m) was higher at MAR (27.8°C) compared to GYR and EGY (22.3 and 18.1°C, respectively). The variations in temperature during the diel cycles were very low, as seen by the standard errors (<0.14°C; Table 1). Z_e was the deepest at GYR (155 ± 9 m), and 92 ± 2 and 72 ± 5 at EGY and MAR, respectively. In terms of depth of TChla maximum (176 m), Z_e (155 m), $Z_{10\%UV\text{-}A}$ (100 to 118 m) and $Z_{10\%UV\text{-}B}$ (21 to 25 m), GYR confirmed its hyper-oligotrophic status (Table 1). From data acquired during the diel cycles, BP values at 5 m depth and integrated data down to Z_e and Z_m were statistically different (higher) only for MAR. BP at 5 m depth was on average 97, 17 and 26 ng C l^{-1} h^{-1} at MAR, GYR

Table 1. Physical, biological and optical characteristics of the sites MAR, GYR and EGY. Z_m: depth of the mixed layer, Z_e: depth of the euphotic zone (1%), $K_{dUV\text{-}B}$ and $K_{dUV\text{-}A}$: diffuse attenuation coefficient for UV-B and UV-A downward irradiances measured at solar noon, $Z_{10\%UV\text{-}B}$ and $Z_{10\%UV\text{-}A}$: corresponding 10% UV-B and UV-A irradiance depths, UV-B and UV-A: 305 and 380 nm, TChla: total chlorophyll *a* (after Ras et al. 2008), BP: heterotrophic bacterial production.Values are mean ± SD, with number of data in parentheses, except $K_{d\lambda}$ and $Z_{10\%\lambda}$ for which the only 2 data available are indicated. Comparison of all variables among the different sites was made using ANOVA, except for $K_{d\lambda}$ and $Z_{10\%\lambda}$ (no statistical test). When a site is significantly different from another ($p < 0.01$), a different superscript letter is assigned

Site	MAR	GYR	EGY
Location	8.4° S, 141.2° W	25.9° S, 114° W	31.8° S, 91.4° W
Date in 2004	26–30 Oct	12–16 Nov	25–30 Nov
Temperature at 5 m (°C)	27.8 ± 0.06 (13)^a	22.3 ± 0.14 (17)^b	18.1 ± 0.03 (9)^c
Z_m (m)	89 ± 9 (13)^a	61 ± 9 (17)^b	32 ± 4 (9)^c
Z_e (m)	72 ± 5 (4)^a	155 ± 9 (4)^b	92 ± 2 (4)^c
$K_{dUV\text{-}B}$ (m^{-1})	0.19, 0.23	0.09, 0.11	0.15, 0.18
$Z_{10\%UV\text{-}B}$ (m)	10, 12	21, 25	13, 15
$K_{dUV\text{-}A}$ (m^{-1})	0.056, 0.066	0.019, 0.023	0.037, 0.044
$Z_{10\%UV\text{-}A}$ (m)	35, 41	100, 118	52, 63
Depth of TChla max (m)	53 ± 15 (6)^a	176 ± 9 (6)^b	73 ± 10 (6)^c
TChla max concentration (mg m^{-3})	0.38 ± 0.05 (6)^a	0.166 ± 0.008 (6)^b	0.25 ± 0.11 (6)^c
BP at 5 m (ng C l^{-1} h^{-1})	97 ± 23 (13)^a	17 ± 7 (17)^b	26 ± 9 (9)^b
Integrated BP to Z_m (mg C m^{-2} d^{-1})	196 ± 25 (13)^a	25 ± 4 (16)^b	22 ± 5 (9)^b
Integrated BP to Z_e (mg C m^{-2} d^{-1})	168 ± 22 (13)^a	65 ± 11 (16)^b	59 ± 11 (9)^b

and EGY, respectively. Integrated data through the euphotic zone were also statistically higher at MAR, despite deeper Z_e at GYR and EGY (Table 1). Microbial populations at MAR were thus slightly more active than at EGY, which is in accordance with the ranges of primary production (PP) rates obtained: 457 to 1146, 159 to 203 and 196 mg C m^{-2} d^{-1} at MAR, EGY and GYR, respectively (Van Wambeke et al. 2008b). Distribution of BP along vertical profiles reflected more or less those of TChla and/or PP (Van Wambeke et al. 2008b), with subsurface peaks at 20 to 40 m at MAR, a regular distribution down to 170 m at GYR, and subsurface peak at 30 to 40 m at EGY. It is worth noting that even with daily-averaged profiles of BP, subsurface peaks were still visible (Fig. 1).

Diel variability of BP

For the 3 sites investigated, coefficient of variation of BP (CV = SD/mean, in percentage) for the whole set of volumetric data at 5 m depth ranged 24, 40 and 36% at MAR, GYR and EGY, respectively. At MAR, BP at 5 m depth increased up to 2.1-fold between 12:00 and 18:00 h, and decreased from 18:00 h to 12:00 h more gradually (increase and decrease rates: 12 ± 3 and 3.7 ± 0.5 ng C l^{-1} h^{-1}, respectively). At GYR, a higher increase (4.7-fold) in activity was recorded later in the day, between 15:00 and 21:00 h (Fig. 2). Again, the decrease was more gradual. Trend at EGY is more difficult to describe because of the longer interval between CTD casts (6 h). However, higher BP values were associated with the late afternoon to midnight period, with up to 1.5-fold variations in 6 h. Considering integrated data, CV of BP integrated down to Z_e ranged 13, 16 and 19% at MAR, GYR and EGY, respectively. CV of BP integrated down to Z_m was close, with slightly higher values at EGY (25%). At MAR, the correlation between BP at 5 m and integrated data was insignificant for integration down to Z_m and slightly significant for integration down to Z_e ($r = 0.61$, $p = 0.02$; Table 2). On the contrary, correlation between BP at 5 m and BP integrated down to Z_m were significant at GYR and EGY ($r = 0.68$, $p < 0.01$ and $r = 0.73$, $p = 0.02$, respectively). However, the correlations were lower or insignificant when relating BP at 5 m with BP integrated down to Z_e at these sites ($r = 0.55$, $p = 0.02$ at GYR and $p > 0.05$ at EGY).

At MAR, the diel variation in volumetric rates of BP at individual depths was not only visible at 5 m depth, but also down to ~50 m depth (Fig. 3), with lower values during morning/noon and increasing values during afternoon/night. Indeed, BP at 5 m depth was significantly correlated with BP at 10 m ($r = 0.77$, $p < 0.01$) and at 15 m ($r = 0.90$, $p < 0.001$) for the whole cycle, as well as with BP at 20 and 40 m the first day ($r = 0.91$, $p < 0.001$ and $r = 0.89$, $p < 0.01$, respectively). However, at GYR the diel variation in volumetric rates of BP at depths other than at the surface was less visible. Succession of max./min. spots were less regular when comparing different depths and successive days, i.e. the first night maximum values occurred between 18:00 and 00:00 h for 5, 40 and depths between 90 and 170 m, and the second night at 21:00 h for 5, 40 and 90 m. However, at 150, 170 and 190 m BP increased slightly during daylight hours, between 09:00

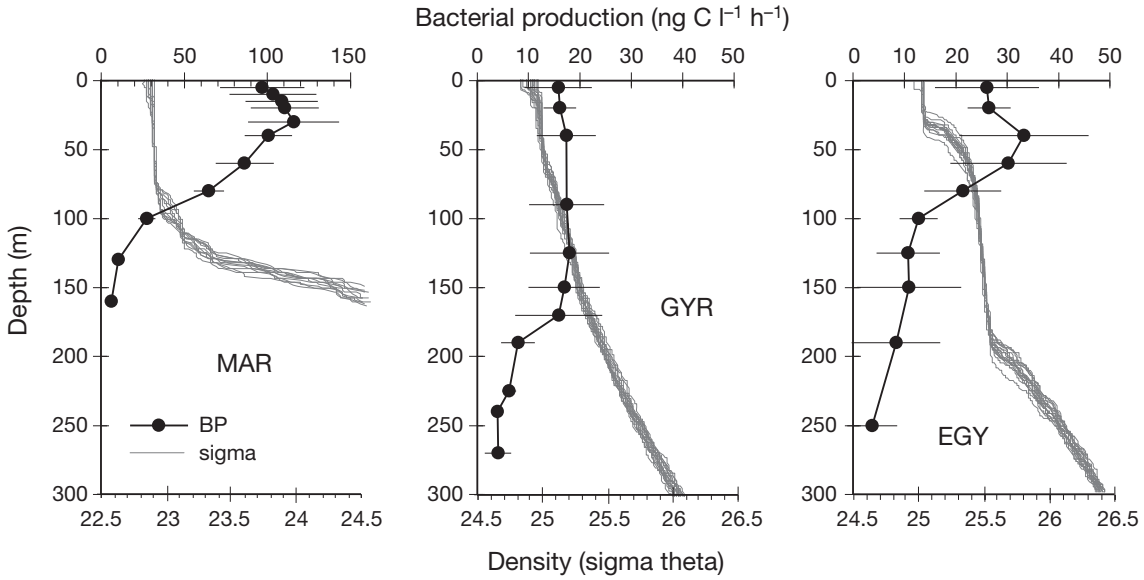

Fig. 1. Vertical profiles of mean heterotrophic bacterial production (BP) at the sites MAR (mean of 9 CTD casts, every 3 h from 27 Nov, 09:00 h to 28 Nov, 09:00 h), GYR (mean of 9 CTD casts: every 3 h from 13 Nov, 18:00 h to 14 Nov, 18:00 h) and EGY (mean of 8 CTD casts every 6 h from 26 Nov, 18:00 h to 28 Nov, 12:00 h, 2004). Error bars = SD. All density profiles (sigma theta, grey lines) from these CTD casts are also indicated

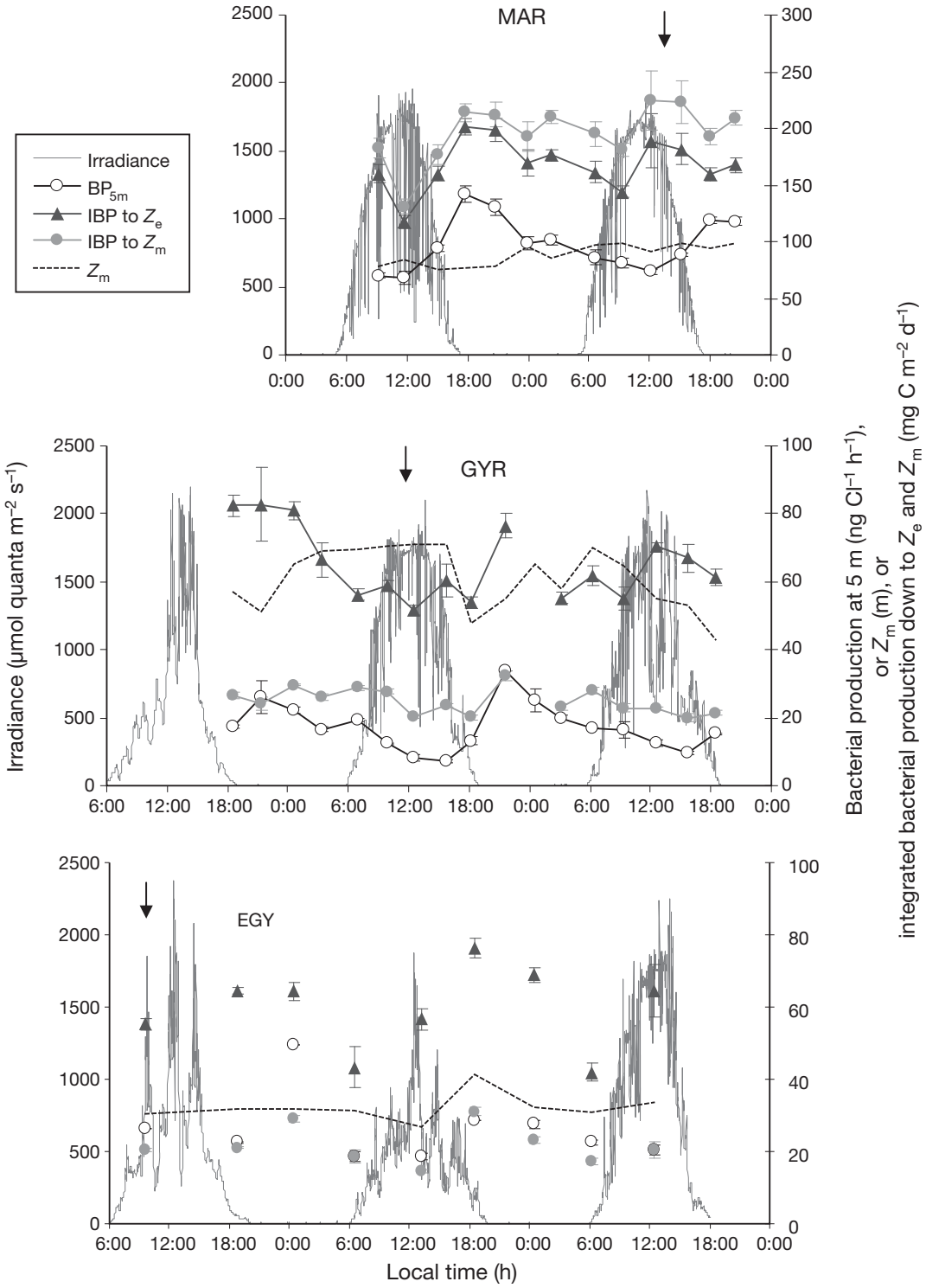

Fig. 2. Evolution of heterotrophic bacterial production at 5 m depth (BP_{5m}), integrated BP down to Z_e (euphotic layer) and down to Z_m (mixed layer), and surface PAR irradiance with time at the 3 sites, i.e. MAR, GYR and EGY. Sampling period and frequency for BP measurements were — MAR: every 3 h from 27 Oct, 9:00 h to 28 Oct, 21:00 h; GYR: every 3 h from 12 Nov, 18:00 h to 14 Nov, 18:00 h; EGY: every 6 h from 26 Nov, 18:00 h to 28 Nov, 12:00 h (plus 1 isolated data point at 9:00 h on 26 Nov, 2004). Z_e was fixed to depth of 1% incident PAR, i.e. 72 m at MAR, 155 m at GYR and 92 m at EGY. Z_m value for integration down to Z_m is the average of the 2 Z_m values obtained for the preceding 3 h period (e.g. to estimate integrated BP at 12:00 h, Z_m was averaged from that obtained at 9:00 h and that obtained at 12:00 h). Arrows: days for which UV-B and UV-A doses were calculated (MAR: 28 Oct, GYR: 13 Nov, EGY: 26 Nov, 2004) (see Figs. 4 & 5). Error bars indicate variability within duplicate samples

Table 2. Coefficient of variation (CV = standard deviation to mean percentage) and correlation coefficients (r) between volumetric rates (bacterial production at 5 m depth, BP_{5m}) and integrated data at the mixed layer (IBP_{Zm}) or euphotic zone (IBP_{Ze}). n: number of data; $^{*}p < 0.05$, $^{**}p < 0.01$, ns: correlation not significant

Site	CV (%)			Correlation, r	
	BP_{5m}	IBP_{Zm}	IBP_{Ze}	$BP_{5m} - IBP_{Zm}$	$BP_{5m} - IBP_{Ze}$
MAR	24	13	13	ns	0.61 (13)*
GYR	40	15	16	0.68 (16)**	0.55 (16)*
EGY	36	25	19	0.73 (9)*	ns

and 18:00 h. Thus, at GYR, diel variations in BP were observed much deeper than at MAR (Fig. 3).

Underwater UV-B and UV-A doses

Daily underwater UV-B and UV-A doses determined at MAR (28 Oct), at GYR (13 Nov) and at EGY (26 Nov) are presented Fig. 4. For the 3 stations, min-

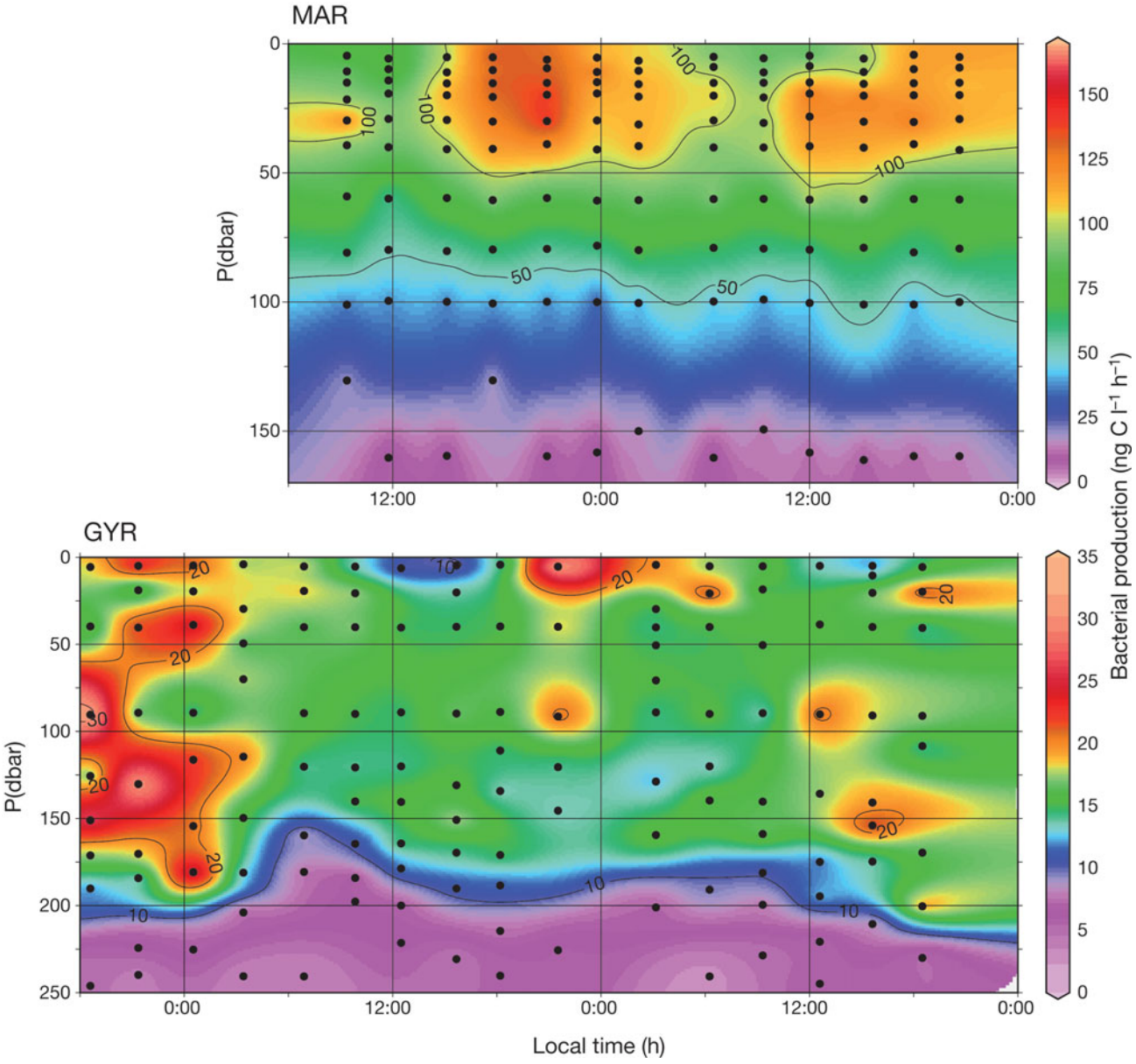

Fig. 3. Contour plots of heterotrophic bacterial production (BP) with time at the sites MAR (0 to 175 m depth) and GYR (0 to 250 m depth). The time periods are as in Fig. 2. Note the different color scales for BP between the 2 sites. Linear color mapping was used for the MAR graph, and non linearity around the value of 15 ng C l^{-1} h^{-1} for GYR to show better color contrasts between 10 and 20 ng C l^{-1} h^{-1} at this site (see color scales)

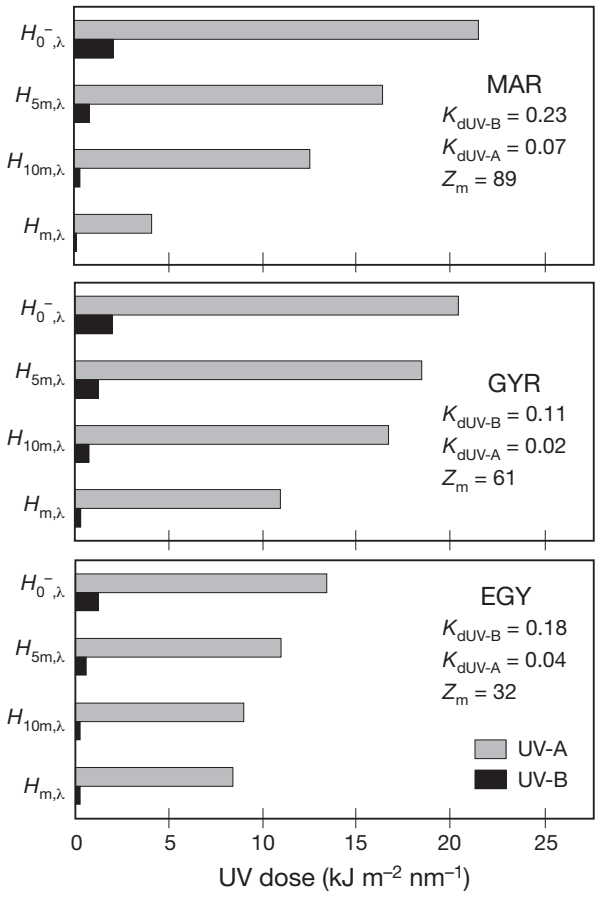

Fig. 4. Daily underwater UV-B and UV-A doses (kJ m^{-2} nm^{-1}) determined at MAR on 28 Oct, at GYR on 13 Nov and at EGY on 26 Nov, 2004. UV-B and UV-A doses received beneath the sea surface ($H_{0^-,UV-B}$, $H_{0^-,UV-A}$), at 5 m depth ($H_{5m,UV-B}$, $H_{5m,UV-A}$) and at 10 m depth ($H_{10m,UV-B}$, $H_{10m,UV-A}$), as well as mean UV-B and UV-A doses received within the mixed layer ($H_{m,UV-B}$, $H_{m,UV-A}$) are represented. Daily doses were obtained by summing doses calculated over tri-hourly exposure periods, i.e. 06:00–9:00 h, 09:00–12:00 h, 12:00–15:00 h and 15:00–18:00 h, and thus correspond to the period 06:00–18:00 h (local time). Average depth of the mixed layer (Z_m in m) and diffuse attenuation coefficient for UV-B and UV-A downward irradiances (K_{dUV-B}, K_{dUV-A} in m^{-1}) measured at solar noon (see Table 1) are given for each station

imal values were found when considering the mean doses within the mixed layer (Fig. 4). At MAR, $H_{0^-,UV-B}$ (2.1 kJ m^{-2} nm^{-1}) and $H_{0^-,UV-A}$ (21.5 kJ m^{-2} nm^{-1}) were slightly higher than those at GYR (2.0 and 20.5 kJ m^{-2} nm^{-1}, respectively) and much higher than those at EGY (1.3 and 13.4 kJ m^{-2} nm^{-1}, respectively). This is explained by high levels of surface solar irradiance at MAR and GYR (sunny days), while the cloud cover encountered at EGY led to a significant decrease of irradiance (Fig. 2). Since the attenuation of UVR into the water column was much lower at GYR (K_{dUV-B} = 0.10 m^{-1}, K_{dUV-A} = 0.02 m^{-1}), UV-B and UV-A doses at 5 and 10 m depth observed at this site were higher than those at MAR. In the same way, the notable discrepancy between MAR and EGY in the doses received beneath the sea surface tended to decrease with depth (even though $H_{5m,\lambda}$ and $H_{10m,\lambda}$ were still higher at MAR), because of a lower UVR attenuation at EGY (K_{dUV-B} = 0.16 m^{-1}, K_{dUV-A} = 0.04 m^{-1}) (Fig. 4). At GYR, $H_{m,UV-B}$ and $H_{m,UV-A}$ were 0.30 and 11.0 kJ m^{-2} nm^{-1}, respectively. These values were considerably higher than those observed at MAR (0.11 and 4.2 kJ m^{-2} nm^{-1}, respectively), for which relatively elevated $K_{d\,\lambda}$ (~0.20 and 0.06 m^{-1}) and Z_m (~89 m) caused a large diminution of doses received within the mixed layer. Interestingly, at EGY, $H_{m,UV-B}$ and $H_{m,UV-A}$ were 0.28 and 8.4 kJ m^{-2} nm^{-1}, respectively, and thus were higher than those recorded at MAR due the relatively small Z_m (~32 m). The latter also contributed to drastically reduce the difference between $H_{10m,\lambda}$ and $H_{m,\lambda}$ (Fig. 4).

Daytime variations of UV-B/UV-A tri-hourly dose ratios (Q in %) are reported Fig. 5. Clearly, Q was

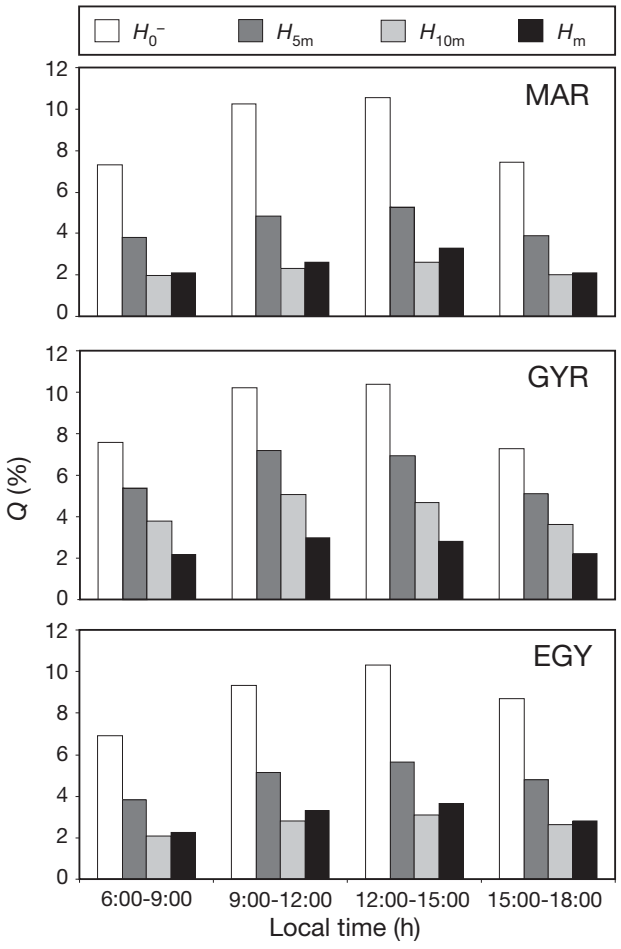

Fig. 5. Daytime variation in UV-B/UV-A tri-hourly dose ratios Q (%) recorded beneath the sea surface ($H_{0^-,UV-B}$ /$H_{0^-,UV-A}$), at 5 m depth ($H_{5m,UV-B}$/$H_{5m,UV-A}$), at 10 m depth ($H_{10m,UV-B}$/$H_{10m,UV-A}$) and within the mixed layer ($H_{m,UV-B}$/$H_{m,UV-A}$) at MAR on 28 Oct, at GYR on 13 Nov and at EGY on 26 Nov, 2004

always higher around solar noon (at the periods 09:00–12:00 h and 12:00–15:00 h) and beneath the sea surface, where it could be as high as 10.5% (MAR: $H_{0^-,\lambda}$, 12:00–15:00 h). Q decreased when moving away from solar noon (in the periods 06:00–09:00 h and 15:00–18:00 h) and with depth. Minimal Q values were obtained at 10 m depth (MAR, EGY) or within the mixed layer (GYR) and could be as low as 2% (MAR: $H_{10m,\lambda}$, 6:00–9:00 h) (Fig. 5).

DISCUSSION

Diel variability in BP has been reported for various marine environments. For instance, Torréton & Dufour (1996) found CV of 10 to 13% in a Tuamotu atoll lagoon (surface layer), and Gasol et al. (1998) 16 to 32% in western Mediterranean coastal waters (surface layer to TChla maximum depth), both estimates were based on the thymidine technique. The latter authors also measured leucine incorporation, which provided a higher variability (CV = 10 to 70%) than that obtained using thymidine. The main feature we observed in the eastern South Pacific was an abrupt increase (2- to 4-fold) in leucine activity at 5 m depth during the afternoon–sunset period and lowest activity around solar noon (between 10:00 and 14:00 h). Previous studies reach no clear consensus about the period in which BP obtains maximal value: at night (Zohary & Robarts 1992), at noon (Gasol et al. 1998) or no significant trend (Torréton & Dufour 1996) with regard to the biogeochemical characteristics of the site and the depth considered. Therefore, the marked diel pattern in BP determined from high-frequency sampling at MAR, GYR and EGY supports the hypothesis that daily variations of some factors controlling BP, either abiotic (solar UVR) or biotic (bottom–up / top–down control) might be particularly pronounced in the eastern South Pacific (Figs. 2 & 4).

Because the SPG likely contained the clearest oceanic waters (Claustre & Maritorena 2003, Morel et al. 2007, Tedetti et al. 2007), we hypothesized that the UV effects could be of great importance and compared surface irradiance and doses received at different depths and within the mixed layer with previous studies. Like Boelen et al. (2000) and Jeffrey et al. (1996), we observed mean UV doses in the mixed layer, lower than UV doses beneath the sea surface (H_{0^-}, see Eq. 3) by a factor ranging between 2 and 18 at the 3 sites investigated. These differences emphasize the importance of taking into account vertical mixing to determine the actual doses received by organisms in the surface oceanic waters. In addition, the high $H_{m,\lambda}$ found in the hyper-oligotrophic part of the SPG (GYR) were explained by a very low UVR attenuation. Although $H_{m,\lambda}$ seems more appropriate than $H_{0^-,\lambda}$ to describe the potential effect of UVR on heterotrophic bacteria in the surface ocean, little data are reported for this parameter. In the tropical Atlantic Ocean, Boelen et al. (2000) measured daily mean UV doses of 0.11 to 0.56 kJ m^{-2} in the mixed layer. Since the latter values were determined from the DNA action spectrum of Setlow (1974) normalized at 300 nm, they may be comparable to our daily $H_{m,UV\text{-}B}$, which ranged from 0.11 to 0.30 kJ m^{-2} nm^{-1}. At GYR, daily doses beneath the sea surface ($H_{0^-,UV\text{-}B}$ = 2.00 kJ m^{-2} nm^{-1}, $H_{0^-,UV\text{-}A}$ = 20.5 kJ m^{-2} nm^{-1}) were of the same order of magnitude than those above the sea surface measured at 305 and 380 nm ($H_{0^+,UV\text{-}B}$ and $H_{0^+,UV\text{-}A}$) in the subtropical Atlantic Ocean (1.7 and 19 kJ m^{-2} nm^{-1}; Obernosterer et al. 2001), in Antarctic waters (1.6 and 25 kJ m^{-2} nm^{-1}; Figueroa 2002) and in the northwestern Mediterranean Sea (1.5 and 21 kJ m^{-2} nm^{-1}; Tedetti & Sempéré unpubl. data). Nevertheless, if the whole UV-B (integration over 280 to 315 nm) and UV-A (integration over 315 to 400 nm) spectra are considered, $H_{0^+,UV\text{-}B}$ and $H_{0^+,UV\text{-}A}$ become much higher. As a matter of fact, in the South Atlantic Ocean (Buma et al. 2001) and in South West New Caledonia (Conan et al. 2008), values measured with the broad band ELDONET radiometer were 40 and 1800 kJ m^{-2} and up to 30 and 2000 kJ m^{-2}, respectively. As a result, the UV-B (at 305 nm) and UV-A (at 380 nm) doses received by heterotrophic bacteria beneath the sea surface and within the mixed layer that we report here for the eastern South Pacific, and more particularly for the SPG, are among the highest doses ever recorded for the marine environment.

The UV-B/UV-A tri-hourly dose ratios (Q in %) presented significant variations during the daytime (Fig. 5), and we tentatively used it as an indicator of daily changes of the balance between DNA damages (CPDs) and repairs (PERs), i.e. when Q increases, the importance of CPDs should increase relative to PERs. The higher 'relative' contribution of UV-B-induced CPDs around solar noon (Fig. 5) could be related to the lower values of BP observed between 10:00 and 14:00 h (Fig. 2). Jeffrey et al. (1996) demonstrated that UV-B was responsible for 85% of the total leucine inhibition (30% relative to dark controls) when heterotrophic bacteria were exposed to full solar radiation in surface waters. From a linear relationship determined experimentally between the CPD formation in naked calf-thymus DNA dosimeters and the UV-B irradiance at 305 nm (Wilhelm et al. 2002), we calculated a mean daily potential production of CPDs within Z_m (regardless of photorepair processes): 420, 800 and 760 CPDs $(Mb\ DNA)^{-1}$ at MAR, GYR and EGY, respectively. These daily potential productions were in the same range as those measured with DNA dosimeters in the surface waters of other oceanic areas: ~500 CPDs (Mb

DNA)$^{-1}$ in the Gulf of Mexico (Jeffrey et al. 1996) and ~1000 CPDs (Mb DNA)$^{-1}$ in the South coast of Curaçao (Boelen et al. 2001, Visser et al. 2002). The period 09:00 h to 15:00 h accounted for 67, 75 and 71% of the daily potential production of CPDs at MAR, GYR and EGY, respectively. Accordingly, these assumed high amounts of UV-B-induced CPDs may lead to the inhibition of BP around solar noon. On the other hand, the lower 'relative' contribution of DNA damages (i.e. lower Q values) at the end of the afternoon (Fig. 5) may explain the abrupt increase or the slower decrease in BP in this period (Fig. 2). In tropical coastal waters, Visser et al. (2002) showed that the inhibition of leucine incorporation in bacterioplankton exposed to full solar radiation strongly increased from 10:00 to 12:30 h or 15:00 h (up to 80% of dark controls) and slightly decreased from 15:00 to 18:00 h. This slower inhibition of leucine incorporation in late afternoon was attributed to PERs. To better appreciate the potential impact of the balance between DNA damages and repairs on the diel variability of BP, at MAR and GYR we examined the relationships between Q and BP for data at 5 m and integrated down to Z_m (EGY was excluded because of the lack of BP data). A significant inverse linear relationship was observed only at GYR between Q_{5m} and BP_{5m} ($r = 0.97$, $p < 0.05$, $n = 4$, data measured at 09:00, 12:00, 15:00 and 18:00 h). The real limits of the mixed layer at GYR (due to micro-stratification; Fig. 1) as well as the limited number of data could partly explain the absence of systematic correlations. In addition, our results illustrate the fact that using *in situ* observations to examine causal relationships between UVR and BP on a daily scale is not easy, particularly when considering cells in their natural environment, i.e. moving within a gradient of light in the mixed layer and influenced also by resource supply and top–down controls.

With regard to phytoplankton resources, if heterotrophic bacteria are closely related to DOC release to satisfy their needs for growth (the first nutrient limiting BP at EGY was labile organic carbon; Van Wambeke et al. 2008a), they should be completely coupled to photosynthesis during the daytime (Marañón et al. 2005). Marked diel cycles in BP are more expected in oligotrophic areas (Gasol et al. 1998, Church et al. 2004) due to this coupling. However, a lag was clearly obtained in the SPG between the process of photosynthesis, PP (as seen from beam attenuation coefficient used as a proxy of biomass changes; Claustre et al. 2008b) and BP (this study). So, it is hypothesized that because of the UV-B-induced production of CPDs around solar noon, there is a delay before BP increases, which is detected when Q starts decreasing, i.e. after 15:00 h (Fig. 5). This hypothesis has also been formulated in other studies dealing with experimental tools, such as the confinement of samples in enclosed quartz tubes subjected to different spectral radiations (Aas et al. 1996, Conan et al. 2008). In the latter study, phytoplankton was more affected by UV-A, whereas it was UV-B for heterotrophic bacteria, suggesting that variations of relative amounts of UV-B and UV-A during the daytime must affect the coupling between phytoplankton/bacteria on a large extent. The lag is also interpreted as a shift in the bacterial metabolism towards expense of energy, because nucleotide excision repair of UV-B-induced DNA damages is energetically expensive (Pakulski et al. 2008).

Regarding regeneration processes, it must be noted that N was the primary limiting nutrient for bacterial production at GYR just before labile organic carbon (Van Wambeke et al. 2008a) and thus regeneration of N could influence BP. Factors limiting bacteria can vary during the day (Kuipers et al. 2000). There was a characteristic and reproducible diel pattern of size spectrum of particles ranging between 0.6 and 4 µm at GYR, with a displacement of its distribution toward higher values around 03:00 h and lower values around 15:00 h (A. Sciandra unpubl. results). This suggests synchronicity in cell division among some cyanobacteria and picoeukaryotes and diel changes of cell physiology, which in turn could lead to diel rhythm in grazing (Christaki et al. 2002) and lysis (Winter et al. 2004, Motegi & Nagata 2007) and, thus, in DOM (including N) regeneration.

Finally, photoheterotrophs could also play a role in diel cycle of BP. First, anoxygenic phototrophic bacteria represented up to 19% of 'heterotrophic bacteria' as counted by flow cytometry just above the depth of TChla at GYR, in conjunction with a peak of bacteriochlorophyll *a* (Lami et al. 2007, Claustre et al. 2008b). Second, *Prochlorococcus* contributed on average to 36% of the sum 'heterotrophic bacteria' + *Prochlorococcus* between 120 and 140 m, and still represented 15% down to 190 m at GYR (Grob et al. 2007). It is thus possible that some patterns in leucine incorporation rates at these very deep layers, not influenced by UV, could be due to the circadian cell cycle of some cyanobacteria able to assimilate leucine (Cottrell et al. 2008, Mary et al. 2008).

The pronounced diel pattern observed in the eastern South Pacific for heterotrophic bacterial production, delayed with that of primary production, suggests a probable interactive control on a daily scale by bottom–up resources (phytoplankton and regenerating micro organisms as producers of labile organic carbon and nitrogen source) and by the quality and intensity of natural solar radiation (UV-B, UV-A and PAR). Further measurements on a daily scale of DNA damages, fluxes of DOM release and regeneration, as well as bacterial re-assimilation of these by-products are necessary in these original, unique, transparent oceanic waters of the South Pacific Gyre to validate these hypotheses.

Acknowledgements. We are grateful to the captain and crew of the RV 'l'Atalante' for their help during the cruise. We warmly thank H. Claustre for leadership of the BIOSOPE project and A. Sciandra for his leadership during the second leg. C. Bournot, D. Tailliez and D. Merien are acknowledged for CTD-rosette operations and data processing. We are grateful to 2 anonymous reviewers for improving the quality of the manuscript. This research was founded by CNRS-INSU, France, as a part of the PROOF – BIOSOPE and UVECO projects.

LITERATURE CITED

Aas P, Lyons MM, Pledger R, Mitchell DL, Jeffrey WH (1996) Inhibition of bacterial activities by solar radiation in nearshore waters and the Gulf of Mexico. Aquat Microb Ecol 11:229–238

Boelen P, de Boer MK, Kraay GW, Veldhuis MJ, Buma AG (2000) UVBR-induced DNA damage in natural marine picoplankton assemblages in the tropical Atlantic Ocean. Mar Ecol Prog Ser 193:1–9

Boelen P, Veldhuis MJ, Buma AG (2001) Accumulation and removal of UVBR-induced DNA damage in marine tropical plankton subjected to mixed and simulated non-mixed conditions. Aquat Microb Ecol 24:265–274

Buma AG, Helbling EW, Boer MK, Villafañe VE (2001) Patterns of DNA damage and photoinhibition in temperate South-Atlantic picophytoplankton exposed to solar ultraviolet radiation. J Photochem Photobiol B Biol 62:9–18

Christaki U, Courties C, Karayanni H, Giannakourou A, Maravelias C, Kormas K, Lebaron P (2002) Dynamic characteristics of *Prochlorococcus* and *Synechococcus* consumption by bacterivorous nanoflagellates. Microb Ecol 43:341–352

Church MJ, Ducklow HW, Karl DA (2004) Light dependence of [^{3}H]leucine incorporation in the oligotrophic North Pacific ocean. Appl Environ Microbiol 70:4079–4087

Claustre H, Maritorena S (2003) The many shades of ocean blue. Science 302:1514–1515

Claustre H, Sciandra A, Vaulot D (2008a) Introduction to the special section bio-optical and biogeochemical conditions in the South East Pacific in late 2004: the BIOSOPE cruise. Biogeosciences 5:679–691

Claustre H, Huot Y, Obernosterer I, Gentili B, Tailliez D, Lewis M (2008b) Gross community production and metabolic balance in the South Pacific Gyre, using a non intrusive bio-optical method. Biogeosciences 5:463–474

Conan P, Joux F, Torréton JP, Pujo-Pay M, Douki T, Rochelle-Newall E, Mari X (2008) Effect of solar ultraviolet radiation on bacterio- and phytoplankton activity in a large coral reef lagoon (southwest New Caledonia). Aquat Microb Ecol 52:83–98

Cottrell M, Michelou VK, Nemcek N, DiTullio G, Kirchman DL (2008) Carbon cycling by microbes influenced by light in the Northeast Atlantic Ocean. Aquat Microb Ecol 50: 239–250

Diaz SB, Morrow JH, Booth CR (2000) UV physics and optics. In: de Mora S, Demers S, Vernet M (eds) The effects of UV radiation in the marine environment. Cambridge University Press, Cambridge, p 35–71

Figueroa FL (2002) Bio-optical characteristics of Gerlache and Bransfield Strait waters during an Antarctic summer cruise. Deep Sea Res II Top Stud Oceanogr 49:675–691

Garcia-Pichel F (1994) A model for internal self-shading in planktonic organisms and its implications for the usefulness of ultraviolet sunscreens. Limnol Oceanogr 39:1704–1717

Gasol JM, Doval MD, Pinhassi J, Calderón-Paz JI, Guixa-Boixareu N, Vaqué D, Pedrós-Alió C (1998) Diel variations in bacterial heterotrophic activity and growth in the northwestern Mediterranean Sea. Mar Ecol Prog Ser 164: 107–124

Gordon H (1989) Can the Lambert–Beer law be applied to the diffuse attenuation coefficient of ocean water? Limnol Oceanogr 34:1389–1409

Grob C, Ulloa O, Claustre H, Huot Y, Alarcón G, Marie D (2007) Contribution of picoplankton to the total particulate organic carbon concentration in the eastern South Pacific. Biogeosciences 4:837–852

Häder DP, Sinha RP (2005) Solar ultraviolet radiation-induced DNA damage in aquatic organisms: potential environmental impact. Mutat Res 571:221–223

Häder DP, Kumar HD, Smith RC (2003) Aquatic ecosystems: effects of solar ultraviolet radiation and interactions with other climatic change factors. Photochem Photobiol Sci 2: 39–50

Jeffrey WH, Aas P, Lyons MM, Coffin RB, Pledger R, Mitchell DL (1996) Ambient solar radiation induced photodamage in marine bacterioplankton. Photochem Photobiol 64: 419–427

Jin Z, Charlock TP, Smith WL Jr, Rutledge K (2004) A parameterization of ocean surface albedo. Geophys Res Lett 31: L22301, doi:10.1029/2004GL021180

Joux F, Jeffrey WH, Lebaron P, Mitchell DL (1999) Marine bacterial isolates display diverse responses to UV-B radiation. Appl Environ Microbiol 65:3820–3827

Kaiser E, Herndl G (1997) Rapid recovery of marine bacterioplankton activity after inhibition by UV radiation in coastal waters. Appl Environ Microbiol 63:4026–4031

Kuhn P, Browman H, McArthur B, St-Pierre JF (1999) Penetration of ultraviolet radiation in the waters of the estuary and Gulf of St. Lawrence. Limnol Oceanogr 44:710–716

Kuipers B, VanNoort GJ, Vosjan J, Herndl GJ (2000) Diel periodicity of bacterioplankton in the euphotic zone of the subtropical Atlantic Ocean. Mar Ecol Prog Ser 201:13–25

Lami R, Cottrell MT, Ras J, Ulloa O and others (2007) High abundances of aerobic anoxygenic photosynthetic bacteria in the South Pacific ocean. Appl Environ Microbiol 73: 4198–4205

Marañón E, Cermeño P, Pérez V (2005) Continuity in the photosynthetic production of dissolved organic carbon from eutrophic to oligotrophic waters. Mar Ecol Prog Ser 299:7–17

Mary I, Garczarek L, Tarran GA, Kolowrat C and others (2008) Diel rhyt*h*micity in amino acid uptake by *Prochlorococcus*. Environ Microbiol 10:2124–2131

Morel A, Gentili B, Claustre H, Babin M, Bricaud A, Ras J, Tieche F (2007) Optical properties of the 'clearest' natural waters. Limnol Oceanogr 52:217–229

Motegi C, Nagata T (2007) Enhancement of viral production by addition of nitrogen or nitrogen plus carbon in subtropical waters of the South Pacific. Aquat Microb Ecol 48:27–34

Myhre G, Stordal F, Johnsrud M, Diner DJ and others (2005) Intercomparison of satellite retrieved aerosol optical depth over ocean during the period September 1997 to December 2000. Atmos Chem Phys 5:1697–1719

Obernosterer I, Ruardij P, Herndl G (2001) Spatial and diurnal dynamics of dissolved organic matter (DOM) fluorescence and H_2O_2 and the photochemical oxygen demand of surface water DOM across the subtropical Atlantic Ocean. Limnol Oceanogr 46:632–643

Pakulski JD, Kase JP, Meador JA, Jeffrey WH (2008) Effect of stratospheric ozone depletion and enhanced ultraviolet radiation on marine bacteria at Palmer Station, Antarctica in the early austral spring. Photochem Photobiol 84: 215–221

Ras J, Claustre H, Uitz J (2008) Spatial variability of phytoplankton pigment distributions in the subtropical South Pacific Ocean: comparison between *in situ* and predicted data. Biogeosciences 5:353–369

Setlow RB (1974) The wavelengths in sunlight effective in producing skin cancer: a theoretical analysis. Proc Natl Acad Sci USA 71:3363–3366

Smith DC, Azam F (1992) A simple, economical method for measuring bacterial protein synthesis rates in sea water using ^{3}H-Leucine. Mar Microb Food Webs 6:107–114

Tedetti M, Sempéré R, Vasilkov A, Charrière B and others (2007) High penetration of ultraviolet radiation in the south east Pacific waters. Geophys Res Lett 34:L12610, doi:10.1029/2007GL029823

Torréton JP, Dufour P (1996) Temporal and spatial stability of bacterioplankton biomass and productivity in an atoll lagoon. Aquat Microb Ecol 11:251–261

Van Wambeke F, Bonnet S, Moutin T, Raimbault P, Alarçon G, Guieu C (2008a) Factors limiting heterotrophic bacterial production in the southern Pacific Ocean. Biogeosciences 5:833–845

Van Wambeke F, Obernosterer I, Moutin T, Duhamel S, Ulloa O, Claustre H (2008b) Heterotrophic bacterial production in the eastern South Pacific: longitudinal trends and coupling with primary production. Biogeosciences 5: 157–169

Visser PM, Jaap Poos J, Scheper BB, Boelen P, Van Duyl FC (2002) Diurnal variations in depth profiles of UV-induced DNA damage and inhibition of bacterioplankton production in tropical coastal waters. Mar Ecol Prog Ser 228: 25–33

Wilhelm SW, Jeffrey WH, Suttle CA, Mitchell DL (2002) Estimation of biologically damaging UV levels in marine surface waters with DNA and viral dosimeters. Photochem Photobiol 76:268–273

Winter C, Herndl GJ, Weinbauer MG (2004) Diel cycles in viral infection of bacterioplankton in the North Sea. Aquat Microb Ecol 35:207–216

Zohary T, Robarts RD (1992) Bacterial numbers, bacterial production, and heterotrophic nanoplankton abundance in a warm core eddy in the Eastern Mediterranean. Mar Ecol Prog Ser 84:133–137